A novel generation of 3D SAR-based passive micromixer: efficient mixing and low pressure drop at low Reynolds number

Vladimir Viktorov and Mohammad Nimafar

Department of Mechanical and Aerospace Engineering (DIMEAS), Politecnico di Torino, Corso Duca degli Abruzzi, 10129, Turin – Italy.

Email address: vladimir.viktorov@polito.it

Abstract

This study introduces a novel generation of 3D splitting and recombination (SAR) passive micromixer with microstructures placed on the top and bottom floors of microchannels called ''*Chain mixer*''. Both experimental verification and numerical analysis of the flow structure of this type of passive micromixer have substantiated to evaluate the mixing performance and pressure drop of the microchannel respectively. We propose here Chain micromixer of two types- Chain 1- and Chain 2- and compare their mixing performance and pressure drop with other micromixers, T-, o- and Tear-drop micromixers. Experimental tests carried out in the laminar flow regime with a low Reynolds number range, $0.083 \leq Re \leq 4.166$, and image-based techniques are used to evaluate mixing efficiency. Also, CFD code, ANSYS FLUENT-13.0 has been used to analyze the flow and pressure drop in the microchannel. Experimental results show that the Chain and Tear-drop mixer's efficiency is very high because of the SAR process: especially, efficiency up to 98% can be achieved at tested Reynolds number. Also results show that Chain mixers have lower required pressure drop in comparison with Tear-drop micromixer.

Keywords:

Chain micromixer

Image-based technique

Mixing index

SAR process

Pressure drop

1. Introduction

Effective mixing is a crucial process in microfluidic systems (Li *et al* 2010) and the potential applications of micromixers are widespread in the industries. Microscale devices have become widely applied in biological systems, medical diagnostic, microreactors for chemical reactions, genetic sequencing, environmental monitoring, MEMS and lab-on-a-chip devices (Bothe *et al* 2011, Yang *et al* 2007, Yang *et al* 2009, Li *et al* 2011).

Indeed, microscale devices propose fundamental advantages compared with conventional macroscale systems because of their small characteristic dimensions (Soleymani *et al* 2008). Microfluidic devices offer many advantages including low energy requirements, faster analysis, reduced reagent and cell consumption, rapid mixing, low cost, rapid heat and mass transfer and portability (Fu *et al* 2007, Sheu *et al* 2012, Song *et al* 2012, Scherr *et al* 2012).

In microfluidic systems, viscosity dominates flow (Wang *et al* 2003, Yang *et al* 2008) and mixing is limited to molecular diffusion due to the laminar nature of microflows (Sinton and Coleman 2005, Hong *et al* 2004, Aubin *et al* 2005) and the flows tend to form a laminate structure instead of a uniform mixture due to the small Reynolds number (Wang *et al* 2011). Hence, the focus on this field of research is to propose a device itself and optimizing the geometry to enhance fluid mixing within the microchannel (Matsuyama *et al* 2010, Shih and Chung 2008, Matsuyama *et al* 2011).

Micromixers reported in the literature can be classified as either active or passive (or static) fluid mixer (Hessel *et al* 2005, Mansur *et al* 2008, Nguyen and Wu 2005, Bockhorn *et al* 2010), depending on how they manipulate the fluid to be mixed (Park *et al* 2010). Active micromixer require external forces (Bhagat and Papautsky 2008), such as periodical variation of pumping capacity, electrokinetic instabilities, acoustically induced vibration, electrowetting-induced merging of droplets, magneto-hydrodynamic action, small impellers, piezoelectrically vibrating membrane or integrated micro valves and pumps (Yang *et al* 2003, Liu *et al* 2003, Glasgow and Aubry 2003). By contrast with active mixers, a passive type requires no external energy and agitation except that associated with producing the flow pressure drop. Passive micromixers are of simple design and in many instances are preferred over active micromixers.

The mixing quality in microscale devices can be characterized using a number of different approaches: a) direct methods of measurement which are usually experimental essence, flow visualization and mixing performance techniques such as acid-base neutralization with an indicator, radioactive tracer and different optical analytical techniques; b) indirect approaches from which the degree of mixing can be quantified include Poincare section analysis, residence time distribution and numerical particle tracking method (Solliec *et al* 2012).

Over the past decade passive micromixers based on various principles have been designed and investigated. Several experimental and numerical investigations have been carried out for different passive micromixers. The mixing of fluids in a passive micromixer is founded on some main principles: a) flow lamination which is used in basic T-mixer and Y-mixer (Kamholz *et al* 1999, Sullivan *et al* 2007, Swickratha *et al* 2009, Bothe *et al* 2011), in mixers with different geometries: zig-zag, square-wave, rhombic and similar (Hossain *et al* 2009), in serial multi-stage and multi-layer mixers (Kwon and Lee 2009, Tofteberg *et al* 2010); b) chaotic mixing by eddy formation, stretching and folding (Kim et al 2007 and 2010, Shih *et al* 2008, Xua *et al* 2011, Cho *et al* 2011, Yu *et al* 2011, Zimmerman and Hassel 2006); c) split-and-recombine concepts (SAR) (Ohkawa *et al* 2008, Lee *et al* 2008, Chen *et al* 2009, Chen et al 2011, Nimafar *et al* 2012).

According to latest investigations, in many cases the micromixers based on SAR principle offer advantages over another types of passive micromixer at small Reynolds number regimes.

Ohkawa *et al* (2008) developed the σ-type plate static mixer with split and inverse recombination progresses for a small Reynolds number less than 10. Lee *et al* (2008) used the mixer based on split and recombination (SAR) with chaotic advection principles for relatively high Reynolds numbers. Chen *et al* (2009) proposed the Tear-drop micromixer and the experimental results demonstrated that mixture uniformity is improved either by accepting a much longer mixing time or by increasing the number of elements, which greatly increases pressure drop.

The high pressure drop is one of the disadvantages of SAR-type micromixer. The prospect of improving the performance of SAR mixers by using of more efficient element geometry is currently central problem. In the present study, a new type of SAR micromixer called the “Chain micromixer” was designed and investigated experimentally to find out the efficiency and numerically to detect the pressure drop, and results were compared with the mixing performance of known T-, O- and Tear-drop micromixers. Two colored water

solutions (blue and yellow) are used for mixing. In all cases (T, O, Tear-drop and Chain mixers), microchannel dimensions are as follows: W=0.4 mm, H=0.4 mm. The aspect ratio of the channel cross-section is unity ($W/H=1$). Channel's length in T, O and Tear-drop are L=21 mm and in Chain mixers are L=25 mm.

2. T-micromixer, O-micromixer and Tear-drop micromixer design

Three basic micromixers were constructed to compare the mixing efficiency of the new microdevice presented in this paper. Figure 1 shows the micromixers which were used in this investigation. T- , O-, Chain1 and chain 2- micromixers were designed and fabricated from plexiglas using a computer milling process. Also figure 1(c) illustrates Tear-drop micromixer which was designed and fabricated from polycarbonate using a computer milling process. The prototypes were fabricated in I.T.D S.n.c. di Depaoli S. & C. (Turin, Italy) using CNC Milling and Engraving Machine P20 S, KUNLMANN (Germany). Geometric characteristics were constant for all prototypes. Two species flow into the microchannel by means of two entrances.

2.1. T-micromixer

The T-micromixer is illustrated in figure 1(a) (Wong *et al* 2004).

The T-micromixer is the simplest microfluidic device with rectangular cross section and consists of two inlets with a straight channel. As shown in figure 1(a), there is no special geometry along the microchannel. The geometry consists of a mixing channel with 21 mm length and 0.4 mm width and depth. All results given here refer to a microchannel with mentioned cross section dimensions.

2.2. O-micromixer

As mentioned in section 2.1, the T-micromixer is the simplest microfluidic device. Hence to show the geometry effect in passive micromixing, O-micromixer (Garstecki *et al* 2006) tested as improved and optimized geometry than T-micromixer. Figure 1(b) illustrates the O-mixer, whose microchannel is divided into two segments: straight channel and O-segment.

Two species flow into the microchannel through the straight section. Subsequently, the stream is divided into two parts and the two streams connect to each other at the end of the O-segment. This splitting and rejoining induce the molecular diffusion effect to enhance mixing efficiency. This process takes place six times along the microchannel.

2.3. Tear-drop micromixer

On the basis of the investigation presented in (Chen *et al* 2009), Tear-drop SAR micromixer was designed and constructed

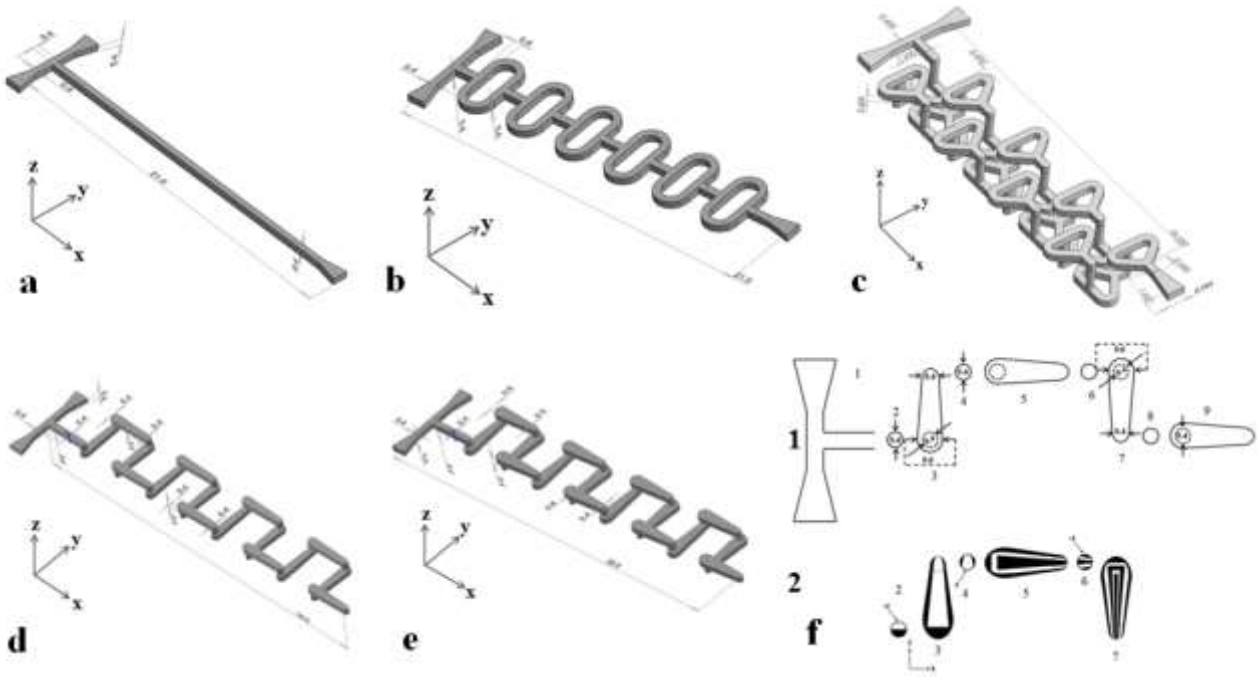

Figure 1. Design of micromixers: a) T-micromixer (Wong *et al* 2004); b) O-micromixer (Garstecki *et al* 2006); c) Tear-drop micromixer (Chen *et al* 2009); d) Chain 1-micromixer; e) Chain 2-micromixer; f) Structural design of Chain 1-micromixer; (1) Chain 1 microchannel segments; (2) Sequential lamination of layers.

with polycarbonate using a computerized milling process. Tear-drop micromixer design is shown in figure 1(c).

Channel width and height are 0.4 mm. As can be seen in figure 1(c), the Tear-drop mixer has a two-layer structure. The modules of the upper layer and the lower layer are connected by simple vertical channels. The inlet to the mixer is designed as a T-junction element (left side of figure).

Device	Description
1	Syringe pump
2	Injection syringe 1
3	Injection syringe 2
4	Transparent tube of syringe 1
5	Transparent tube of syringe 2
6	Micromixer
7	Microscope
8	Outlet tube

Figure 2. Test bench layout.

This method of splitting and recombining the flow provides a way of increasing the number of fluid layers. It is founded that the efficiency of this mixer is high and also the required pressure drop is great.

3. Mathematical Model

At the continuum level, constitutive governing equations are described with a set of conservation equations.

1- Continuity (conservation of mass)

2- Navier-Stokes equation or Newton's second law (conservation of momentum)

Solving above equations will result in two variables: the velocity ***V*** and the pressure ***P***. These equations are formulized for a solo phase of homogenous composition.

Continuity (conservation of mass):

$$\frac{\partial \rho}{\partial t} + \nabla(\rho \vec{V}) = 0 \tag{1}$$

Navier-Stokes equation:

$$\frac{\partial \rho \vec{V}}{\partial t} + \nabla(\rho \vec{V}\vec{V}) = -\nabla p + \nabla\left\{\mu\left[(\nabla \vec{V} + \nabla \vec{V}^{T}) - \frac{2}{3}\nabla \vec{V} I\right]\right\} \tag{2}$$

Where ρ denotes density, μ the viscosity and p the pressure.

Computational fluid dynamics software, ANSYS-Fluent 13.0 was used to solve the governing equations (1) and (2). In this study the value of the ρ and μ are 998 kg m^{-3} and 0.00089 kg $m^{-1}s^{-1}$ respectively. Also some assumptions such as steady-state flow, no-slip conditions and incompressible fluid are proposed. Required information for numerical calculations are as follows: solver Fluent13.0.0, Mesh nodes for 1) T =280000 hexahedral cells; 2) O =220480 tetrahedral cells, 3) Tear-drop=379670 hexahedral cells; 4) Chain 1=218810 hexahedral cells and 5) Chain 2=259870 hexahedral cells, Under Relaxation Factor: a) Pressure=0.3; b) Density=1; c) Body Force=1 and d) Momentum=0.7, and Monitor Convergence Criteria a) Continuity= 1e-20; b) x-velocity= 1e-20; c) y-velocity= 1e-20; d) z-velocity= 1e-20. Also the boundary conditions used in this investigation are as follows: inlet 1: mass flow inlet (kg/s); inlet 2: mass flow inlet (kg/s); outlet: pressure outlet (Gauge Pressure (Pascal) is equal 0).

4. Materials and method

The test bench layout used for this experimental investigation is shown in figure 2.

Microscope: The microscope used during the mixing process is a Veho model VMS-004D-400x USB microscope, with 400X magnification, 2 Megapixel Cmos lens (interpolated) and measurement software.

Syringe pump: The syringe pump used in this study is a KDS 210 series. The flow rate range for this instrument is from 0.1 µl/hr (10µl syringe) to 506 ml/hr (60 ml syringe) with errors less than 1% (according to the catalog).

Dye: For visualization the flow, blue and yellow food dyes are diluted in water.

4.1. Chain-micromixers design

A novel generation of 3D passive micromixer concept is introduced. This type of micromixer called the ‘’Chain micromixer’’ which is based on the SAR process, meaning that the two fluids to be mixed are split and recombined to optimize the diffusion process. The main working principle for this type of microchannel is to make 90º rotation of a flow, folding the stream and then split and recombine the flow to enhance the

efficiency of the microchannel. This process is repeated during the microchannel until achieving the desired degree of mixing. Chain 1- and Chain 2- micromixers were designed and fabricated from plexiglas using a computer milling process. As illustrated in figure 1(d) and (e), the flow follows a 3D path along the microchannel.

Figure 1(d) illustrates the Chain 1-micromixer. As shown in figure 1(d), after each vertical part (z direction), the diameter of the new section is 0.6 mm and extended 0.2 mm rather than the outlet of vertical part (0.4 mm). This characteristic

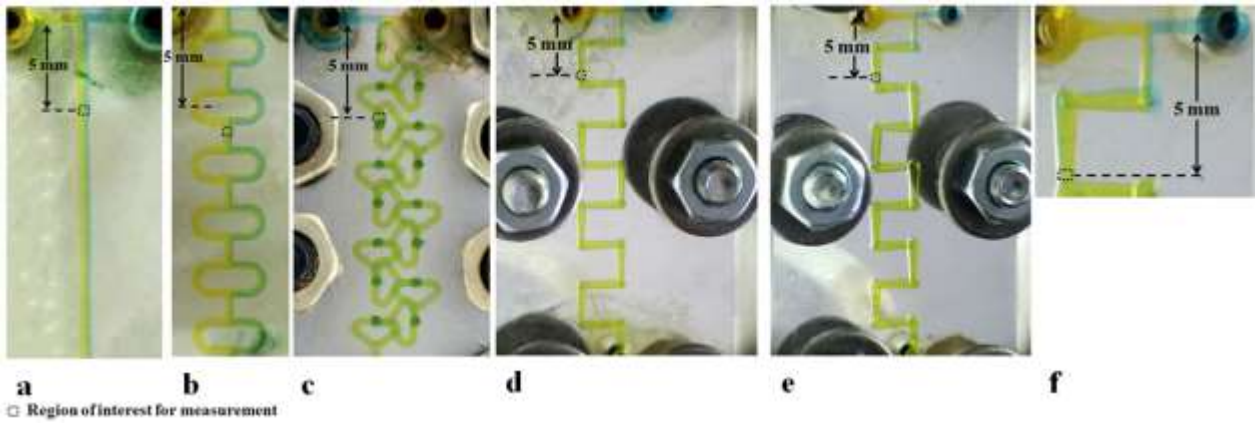

Figure 3. Micromixers after filling: (a) T-micromixer; (b) O-micromixer; (c) Tear-drop micromixer; (d) Chain 1-micromixer; (e) Chain 2-micromixer; (f) Chain 2-micromixer, inlet part to 5 mm.

of the geometry causes the splitting of the flow in the inlet of new part (figure 1(f), segments 3, 5, 7 and 9) and in the central part of the segment the recombination effect takes place. At the outlet of the segment, the diameter is again 0.4 mm like the vertical part (figure 1(f), segments 3, 5, 7 and 9). Indeed, after extension in the inlet, the flow getting constricted while going across these parts and the maximum constriction occurs at the outlet of this section. The maximum width of the microchannel is 0.6 mm and reduces during this part to minimum value of 0.4 mm.

As in the case of the Chain micromixer depicted in figure 1, two mixing flows meet along the entrance microchannel and move along the entrance part until reach to the vertical part. In the vertical part the flow moves in –z direction. At the end of the vertical channel the stream reaches the first chain element.

The black color flow is then moved against a wall and the white color flow is moved to central part of the chain segment (3). In this way the flow is first splitted and then recombined into three layers flow, white and

two black flows, as depicted in figure 1(f) segment (4). After reaching to the vertical part, where these layers rotate 90º, in the next mixer segment (5) and five layers are created as illustrated in figure 1(b) segment (6). By the same procedure, after segment 7 nine flow layers are formed. This process continues to the end of the Chain-micromixer. In fact, splitting and recombination processes cause large number of different layers and with increasing the layers, thickness of the layers will be smaller and the thickness of the poor mixed zone will be shorter and part of this zone moves to other mixed zone and this process proceed. This property enhances the mixing efficiency and homogeneity. Therefore with folding, expansion and constriction along with splitting and recombination, mixing can be improved significantly.

Figure 1(e) illustrates the Chain 2 mixer which differs only by one parameter from the Chain 1 mixer. As shown in figure 1(e), after each vertical part (z direction), the diameter of the new section is 0.8 mm and extended 0.4 mm rather than the outlet of vertical part (0.4 mm).

Experimental and numerical tests were performed for ‘’Chain 1and 2’’ micromixers.

5. Experimental procedure

Experimental tests were performed using a microscope with high speed image acquisition. Colored water was used as mixing species in all tests; specifically, blue and yellow solutions were produced by blending 1 gram powder in 0.5 liter water. As mentioned before, blue and yellow food dyes are diluted in water as the mixing flow in experimental tests. The mass flow rates of the mixing species are controlled by means of a programmable syringe pump (KDS 210 Series, KD Scientific). The T-, O- and Tear-drop micromixers studied in this paper are shown in figure 3(a, b and c).

During the mixing process, several pictures were taken with the microscope from the entrance area to the end of the channel. This was repeated for all Reynolds numbers and also for Chain mixers which was used in this study. The Chain 1- and Chain 2-micromixers studied in this paper are shown in figure 3(d and e).

Image-based techniques were used to evaluate the mixing performance of the prototypes, and the gray scale value was applied for post processing. To analyze the image, captured color images were converted into gray scale images. To convert any color to gray scale representation of its luminance, first one must obtain the value of its red, green and blue (RGB) primaries in linear intensity encoding. Then add together 30% of the red values, 59% of the green values, and 11% of the blue values. In this study Adobe Photoshop software

version 12.0, is applied to convert the colored images to gray-scale images. This technique (gray scale value) is useful for highlighting regions of interest, especially the concentration field in the micromixer (Nguyen 2008).

6. Post Processing

To evaluate the standard deviation of concentration, mixing index and efficiency of the prototypes, three kinds of Matlab M-file code were written (PDF1, PDF2 and Efficiency). Data were analyzed using the following procedure.

The microscope's Cmos lens provide bit depth of 8 and an 8-bit depth describes 256 (2^8) different gray levels. If

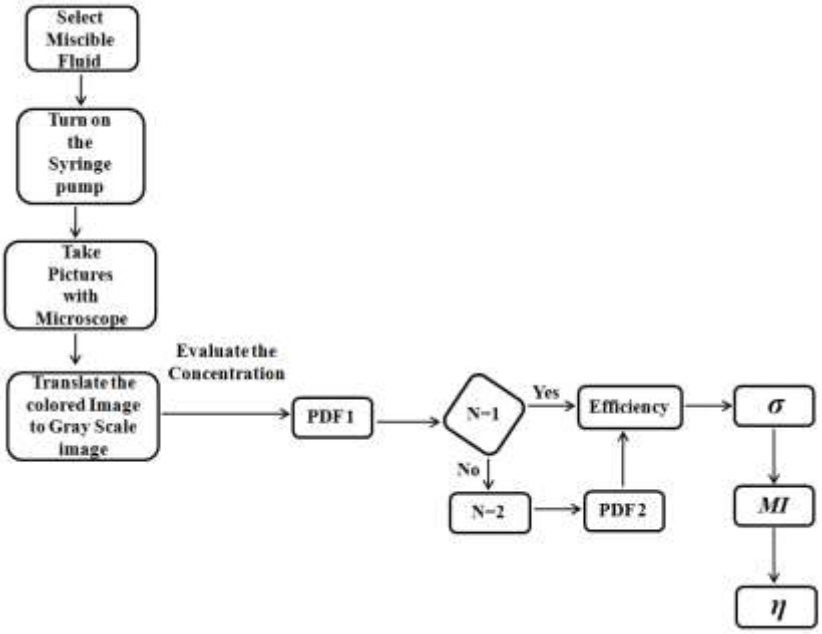

Figure 4. Flow chart for experimental analyzing.

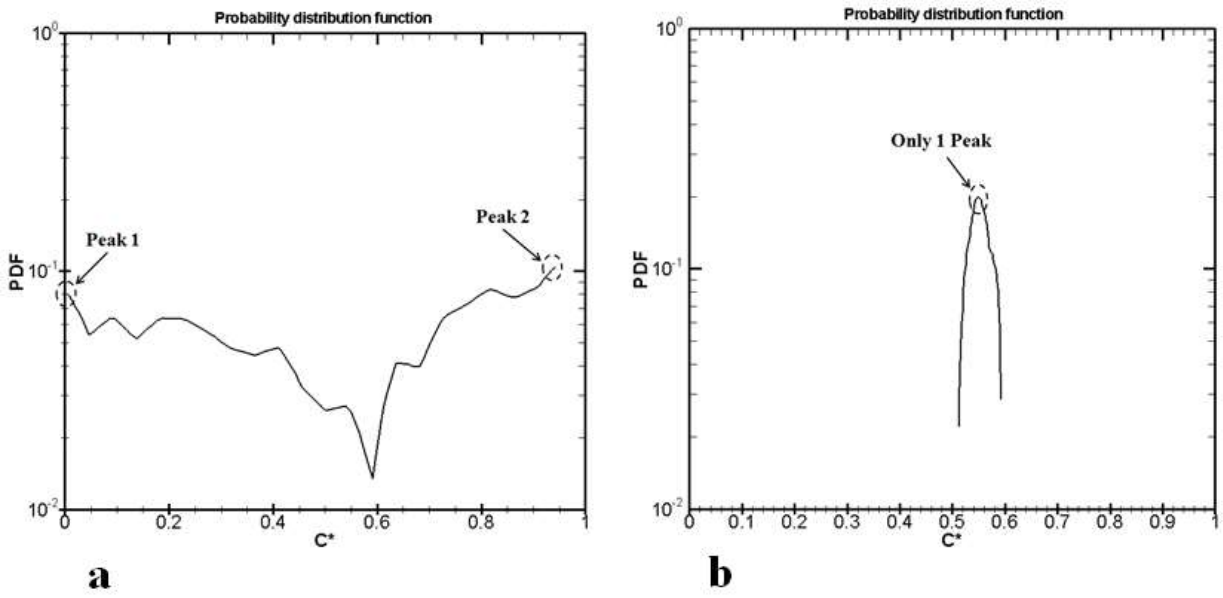

Figure 5. (a) *PDF* in chain 2-micromixer at Re = 4.166, entrance region; (b) *PDF* in Chain 2-Micromixer at *Re* = 0.416, after 21 mm.

the species are black and white, the gray level varies from 0 to 255 respectively and there is no need to calibrate the program which shows that concentration varies from 0 to 1 in the PDF diagram. Since the species are yellow and blue, gray level does not vary from 0 to 255 and gray level range reduces (for example: between 60 and 220). Hence, it does need to be calibrating that concentration varies from 0 to 1 in the PDF diagram. For this purpose, in the program code we put for example 60 (instead of 0) as a minimum value and 220 (instead of 255) as a maximum value. This procedure occurs in PDF 2. Therefore the program (PDF 1) after calibration is ready to analyze the Gray scale image.

Figure 5 presents the probability distribution function in terms of concentration which was calculated and plotted by Matlab program codes (PDF 1 and 2). Subsequently, probabilities for different concentration values and for various Reynolds numbers were calculated and plotted for Chain prototypes.

The two species are not mixed in the entrance region of the micromixers, where there are two predominant concentration values resulting in two separate peaks as shown in figure 5(a). In a region of well-mixed fluids, there is one predominant concentration and this value depends on the color of the mixing process that can be seen as the best issue, resulting in a single peak as illustrated in figure 5(b).

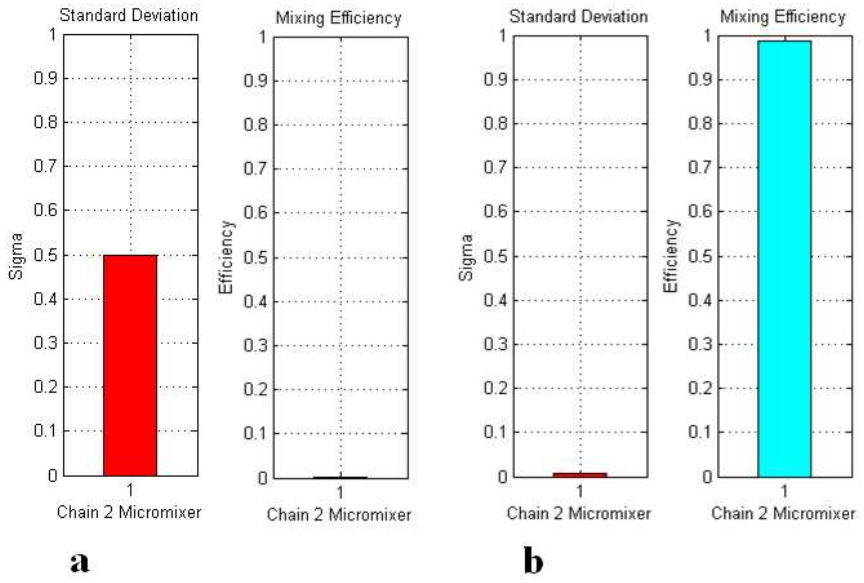

Figure 6. Chain 2-Micromixer analysis: (a) Re = 4.166, entrance region; (b) Re = 0.416, after 21 mm.

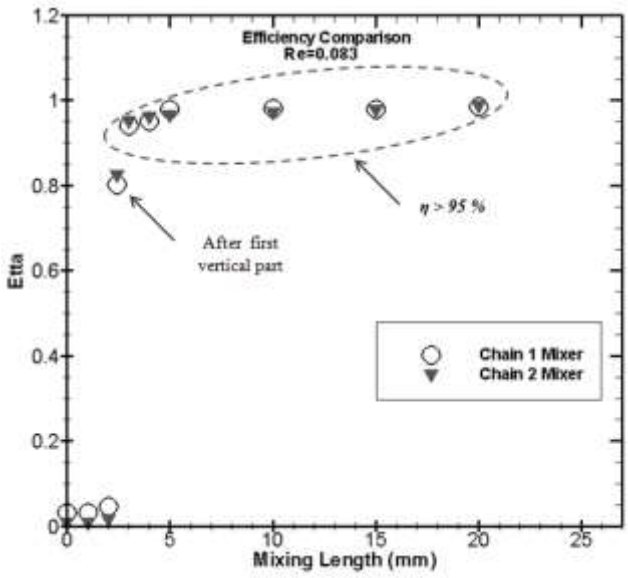

Figure 7. Comparison of η in Chain 1 and Chain 2 mixers at *Re* = 0.083.

The homogeneity can be represented as the standard deviation (variance) of the concentration:

$$\sigma = \sqrt{\frac{1}{N}\sum_{i=1}^{N}\left(C_i^* - \bar{C}^*\right)^2 * PDF_i} \quad (3)$$

Where C^* is the normalized concentration and $\overline{C^*}$ is the expected normalized concentration (depends on the color that can be seen as the best result). The standard deviation can be normalized again by the mean concentration to evaluate the mixing index (MI):

$$MI = \sqrt{\frac{1}{N}\sum_{i=1}^{N}\left(\frac{C_i^* - \bar{C}^*}{\bar{C}^*}\right)^2 * PDF_i} \quad (4)$$

The mixing indexes (MI) are 1 and 0 for the unmixed case and well-mixed case, respectively. Mixing efficiency can be defined through equation 5:

$$\eta = 1 - MI \quad (5)$$

If the two species are fully mixed, mixing efficiency is 1 (100%). An efficiency between 80% and 100% is acceptable for mixing process applications (Nguyen 2008).

At the starting point where two fluids join together, the standard deviation is high, mixing index is 1 (or approximately 1) and efficiency is 0% (or approximately 0%). Figure 5(a) illustrates the Chain 2-mixer's concentration at the entrance region at *Re*=4.166, while figure 6(a) shows σ and η at the same Reynolds number, where efficiency is 1%. Figure 5(b) depicts the Chain 2-mixer's concentration at the outlet region at Re=0.416, while figure 6(b) shows σ and η under the same Reynolds number, where efficiency is 98% (η>80%).

These processes continue for Reynolds numbers of 0.083, 0.832, 1.666 and 4.166 for all prototypes.

The experimental errors depend on the quality of the pictures and selecting the region of interest in microchannel which would be considered in the post processing step. The maximum measurement error could be seen when the flow is far from the mixed condition, for example, in the entrance region or in the case of using the poor performance mixer.

7. Results and discussion

In this study, the effects of geometry and various Reynolds numbers on flow field and mixing characteristic along the Chain microchannels are examined and mixing efficiencies are compared with T-, O- and Tear-drop micromixers. Five different flow rates (ml/min) were considered. The corresponding average flow

velocity and Reynolds numbers are shown in table 1 are calculated for the first part of the devices in all micromixers after two species reach together. In all tested micromixers, size of the channel width is 0.4 mm and also channel height is 0.4 mm in the first part (T junction part).

Then, the effects of various Reynolds numbers and geometry on pressure drop were examined numerically using CFD code, ANSYS FLUENT-13.0. Henceforth, numerical results for Chain microchannels are compared with well-known basic microchannels.

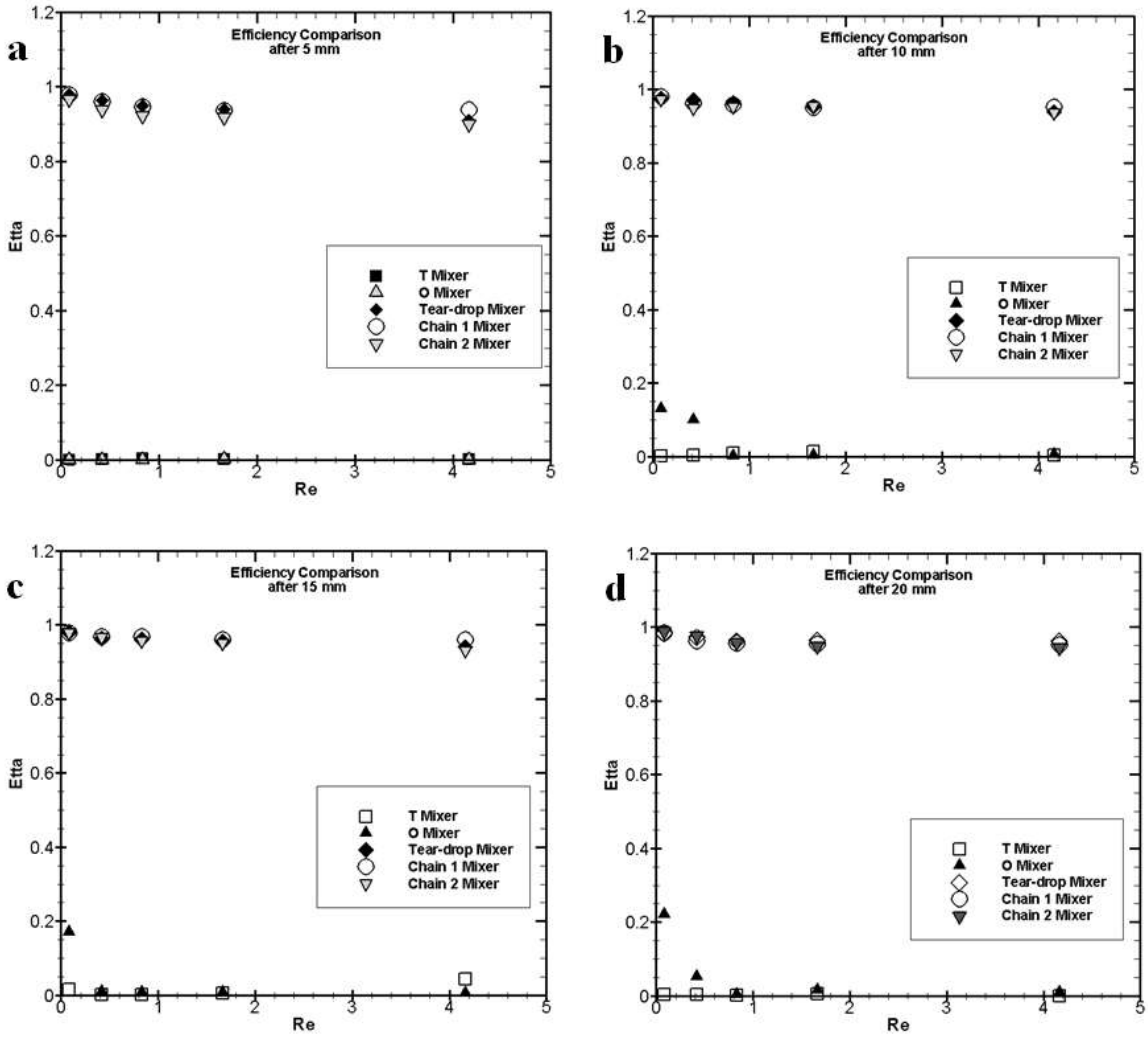

Figure 8. Comparison of η in terms of *Re*: (a) after 5 mm; (b) after 10 mm; (c) after 15 mm; (d) after 20 mm.

Table 1. Flow rate, *Re* and velocity values during experimental and numerical investigation.

Q_v (ml/min)	Q_m (kg/s)	V (mm/s)	*Re*
0.001	$1.66*10^{-8}$	0. 1	0.083
0.005	$8.31*10^{-8}$	0. 5	0.416
0.01	$1.66*10^{-7}$	1	0.832
0.02	$3.32*10^{-7}$	2	1.666
0.05	$8.32*10^{-7}$	5.2	4.166

7.1. Experimental Analysis

Results of experimental investigation of the chain micromixers are presented below. PDF software and equations (3), (4) and (5) are used to calculate and plot standard deviation of concentration $\boldsymbol{\sigma}$, mixing index ***MI*** and efficiency $\boldsymbol{\eta}$ at different *Re* along the microchannel. The mixing efficiency is quantified by evaluating the variance of the mixture in a cross-section which is normal to the flow direction by equation (3). The variance can be normalized again by the mean concentration to get the Mixing Index by equation (4). Afterward, the efficiency can be defined based on the Mixing Index by equation (5).

Figure 7 illustrates the efficiency versus the distance from the inlet section in Chain 1 and Chain 2 mixers at Re=0.083.

As shown in figure 7, after 5 mm in Chain 1 and Chain 2, the efficiency under *Re*=0.083 is more than 95% and acceptable for mixing processing. Also, it could be seen after first vertical part, the efficiency reach to 80% which shows the effect of split and recombination in the micromixing application.

Figure 8 illustrates efficiency versus Reynolds number for different micromixers. As the diagram shows, efficiency decreases as Reynolds number increases and vice versa. This phenomenon related to the residence time distribution in the microchannel. When Reynolds number is very low, two species have more time for mixing and by increasing the Reynolds number (velocity) the residence time decreases.

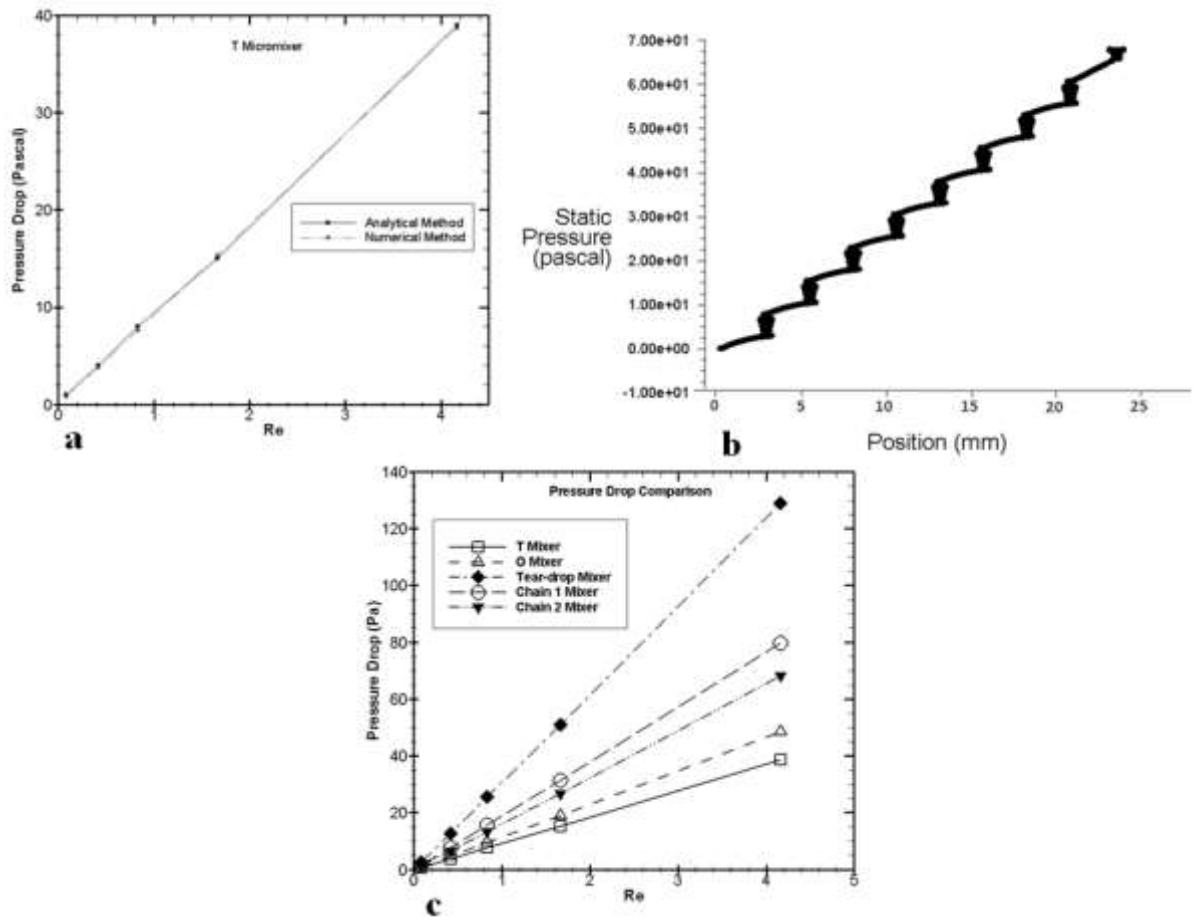

Figure 9. : (a) Comparison of Pressure Drop between Analytical Method and Numerical Method for the T Mixer; (b) Pressure drop in Chain 2 micromixer during microchannel at *Re =4.166*; (c) Pressure Drop Comparison at different Re.

Hence, in the *Re* number range Re < 1, micromixer efficiency is higher than in the range 1< Re < 5.

After 5 mm, Tear-drop-, Chain 1 and Chain 2-mixers efficiencies are acceptable, while in other prototypes the degree of mixing is low (η < 25%), demonstrating the effect of splitting and recombination on micromixer efficiency.

Results for the efficiency comparison after 10 mm are shown in figure 8(b). Since the operations of T- and O-mixers for the Reynolds range (0.083< Re < 4.166) were found to be invalid for efficient mixing, it is evident that mixers based on the SAR process effects demonstrate efficient mixing at this Reynolds number range. Also, it could be seen after 10 mm the Chain and Tear-drop mixers efficiencies are over 90% at all tested Reynolds numbers, which shows that the SAR effect is significant in short distance.

The experimental results about the level of mixing after 15 mm are displayed in figure 8(c). As could be seen again, without SAR process, there is poor mixing condition in T- and O-microchannels. It is obvious that the separation of mixture's layers and recombining them again due to the geometrical effects leads to fast mixing at low Reynolds number range.

Figure 8(d) displays the efficiency comparison at the end regions of the mentioned micromixers and an overview on the effects of revenue and design on mixing efficiency is presented. Not far from a lamination concept, a novel generation of the 3D passive micromixers, has a significant efficiency and it could be seen the efficient mixing from microchannel. As depicted in figure 8(d), not only there is acceptable and great efficiency at Re < 1, but also is evident at 1< *Re* < 4.166, efficiencies are acceptable in Tear-drop, Chain 1- and Chain 2- mixers. It is possible to increase the Reynolds number to achieve the faster and complete mixing in Chain micromixer and also reduce the microchannel length.

This new concept for multi-laminated layers and SAR process that occurs in Chain 1 and Chain 2- micromixers can lead to enhancing the mixing speed and this characteristic is essential and applicable to micro technology.

7.2. Numerical Simulation

To analyze the flow and pressure drop in the microchannel, CFD code, ANSYS FLUENT-13.0 has been used. The Fluent

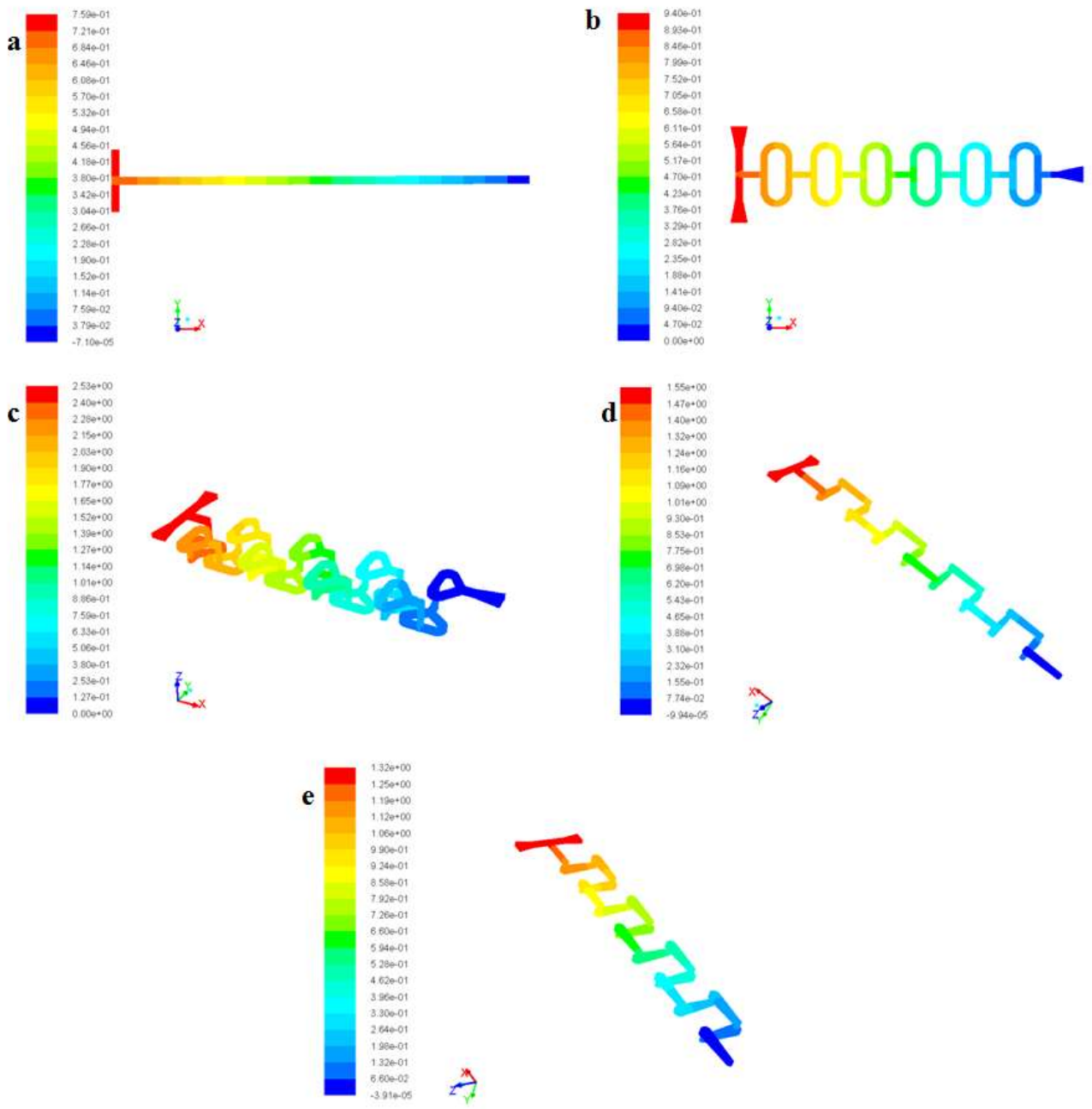

Figure 10. Pressure drop at *Re* = 0.083: (a) T-micromixer (b) O-micromixer (c) Tear-drop micromixer (d) Chain 1- micromixer (e) Chain 2- micromixer, Pressure drop (Pa).

solves the continuity and Navier-Stokes equations in steady condition.

To validate the approximation accuracy of the solver and assumptions which applied in this study, analytical method compared with numerical method in T mixer.

To find out the pressure drop in analytical method, Darcy's law is applied.

$$\frac{dp}{dx} = \frac{-32\mu v}{d^2} \tag{6}$$

Where μ denotes the viscosity, v the velocity, p the pressure, and d the hydraulic diameter of the microchannel.

Figure 9(a) demonstrated the differences between two mentioned methods are very small and negligible. Hence, CFD calculations with ANSYS FLUENT 13.0 under the mentioned assumptions are reliable to find out the pressure drop. Therefore, numerical technique is applied to detect the pressure drop during the microchannel which was found to be accurate in comparison with analytical method.

Figure 10 illustrates the contour of pressure during the five passive micromixers at *Re =0.083.* As could be seen, pressure drops in Chain 1- and Chain 2 microchannels are 1.55 and 1.32 Pascal respectively, while the pressure drops are 2.53, 0.94 and 0.75 in Tear-drop-, O-and T- mixers respectively. It shows that

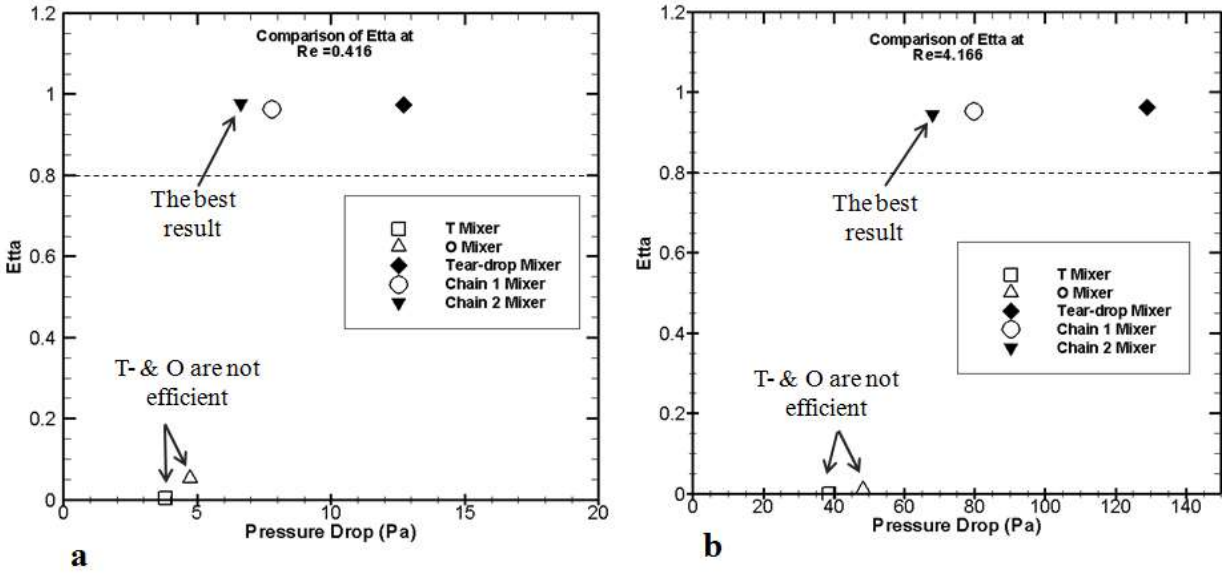

Figure 11. Efficiency Comparison versus Pressure Drop: a) Re=0.416; b) Re=4.166.

Tear-drop micromixer has a higher pressure drop than the other tested microdevices at *Re =0.083*.

Also, for example figure 9(b) illustrates the pressure drop in Chain 2 micromixer is 68.1 Pa at *Re =4.166*. In comparison with figure 10 (e), it could be found that pressure drop increases as Reynolds number increases.

Figures 9(c) and 11 demonstrates that Tear-drop micromixer's pressure drop is significantly higher than that of the Chain 1, Chain 2, T- and O-micromixers at all tested Reynolds numbers.

According to figures 8(d), 9(c) and 11, in comparison with other Reynolds numbers it could be found that with increasing the Reynolds number, efficiency decreases and pressure drop increases.

The Chain mixers have been designed with the goal of maximizing the mixing efficiency and minimizing the pressure drop associated with the energy consumption. As is evident from the foregoing, the mixing efficiency of the Chain mixers is practically identical with those of the Tear-drop mixer while the pressure drop at the Chain mixers is approximately two times less than it is at the Tear-drop mixers. The developed Chain micromixers offer major advantages by virtue of their higher fluid conductivity of the Chain mixer element in comparison with the Tear-drop mixer element. Also figure 9(c) depicts that in all of the Reynolds numbers range, the required pressure drop in Chain 2 is less than Chain 1. This is a good result that with the same (or higher) efficiency the required pressure drop decreases. Hence, these two new geometries satisfy both of targets in micromixer design which have higher mixing efficiency and lower pressure drop (in comparison with Tear-drop mixer).

9. Conclusion

This paper introduced a novel generation of 3D splitting and recombination passive micromixer called ‘’*Chain micromixer*’’. Mixing characteristics of two species are elucidated via experimental and numerical studies with various inlet flow rates (velocities) and results compared with the previous well-known micromixers. Chain 1 and Chain 2 micromixers are designed and fabricated from plexiglas using a computer milling process and the flow follows a 3D path along the microchannel. It was found that mixing performance is significantly affected by the split and recombination (SAR) flows and depends on Reynolds number (inlet velocities).

Experimental results illustrate that the micromixers with SAR process like Chain 1-, Chain 2 and Tear-drop micromixers have outstanding mixing efficiency than those without SAR characteristic. Indeed split and recombine (SAR) structures of the flow channels result in the reduction of the diffusion distance of two fluids and after a short distance from inlet high mixing efficiency can be achieved.

In Chain micromixers, after each vertical channel, the diameter of the new section is extended 0.2 mm or 0.4 mm in Chain 1- and Chain 2 – micromixers respectively rather than the outlet of vertical part (0.4 mm). At the outlet of this part, the diameter is again 0.4 like vertical part. Indeed, after extension in the inlet, the flow

getting constricted while goes across these parts and the maximum constriction occurs at the outlet of this section and mentioned properties cause the homogeneity in the mixed layers. Therefore splitting and recombination along the Chain 1- and Chain 2- micromixers and repeating these processes lead to significantly improved mixing and it was obvious that the efficiency of Chain 2 is the same as Chain 1 at each desired region. Also it could be found that with increasing the Reynolds number, efficiency decreases and pressure drop increases. As well as the efficiencies of Chain mixers and Tear-drop mixer are almost quite the same at each desired region, the required pressure drop in Chain mixers is approximately two times less than pressure drop in Tear-drop mixer. Also in Chain mixers, required pressure drop in Chain 2 is less than Chain 1. This is a good particular result that with higher efficiency the required pressure drops decreases. Hence, this new geometries satisfies both of targets in micromixer design which have higher mixing efficiency and lower pressure drop in comparison with Tear-drop.

These results open the new operating windows for rapid mixing in the microchannel to overcome the fluid mixing which strongly limited to laminar regime with lower required pressure drop. For our future work, the optimization of the Chain mixer with development of new designs would be considered and it is expected to find out high efficiency and low pressure drop in upcoming Chain micromixers.

References

Aubin J, Fletcher DF and Xuereb C 2005 Design of micromixers using CFD modelling *Chemical Engineering Science 60* 2503-2516 doi: 10.1016/j.ces.2004.11.043

Bhagat A A S and Papautsky I 2008 Enhancing particle dispersion in a passive planar micromixer using rectangular obstacles *J. Micromech. Microeng.18* 085005 9pp doi:10.1088/0960-1317/18/8/085005

Bockhorn H, Mewes D, Peukert W and Warnecke H J 2010 Micro and Macro Mixing: Analysis, Simulation And Numerical Calculation *Heat and Mass Transfer (Springer)* ISBN: 3642045480

Bothe D, Lojewski A and Warnecke H J 2011 Fully resolved numerical simulation of reactive mixing in a T-shaped micromixer using parabolised species equations *Chemical Engineering Science 66* 6424-6440 doi: 10.1016/j.ces.2011.08.045

Chen J J, Lai Y R, Tsai R T, Lin J D and Wu C Y 2011 Crosswise ridge micromixers with split and recombination helical flows *Chemical Engineering Science 66* 2164-2176 doi: 10.1016/j.ces.2011.02.022

Chen Z, Bown M R, Sullivan B O, MacInnes J M, Allen R W K, Mulder M, Blom M and van't Oever R 2009 Performance analysis of a folding flow micromixer *Microfluid Nanofluid 6*:763–774 doi: 10.1007/s10404-008-0351-z

Cho H H, Kim B S, Kwak B S, Shin S, Lee S, Kim K M and Jung H I 2011 Optimization of microscale vortex generators in a microchannel using advanced response surface method *International Journal of Heat and Mass Transfer 54* 118-125 doi:10.1016/j.ijheatmasstransfer.2010.09.061

Fu L M and Lin C H, 2007 A rapid DNA digestion system, *Biomed Microdevices 9* 277-286 doi: 10.1007/s 10544-006- 9036-0

Garstecki P, Fuerstman M J, Fischbach M A, Sia S K and Whitesides G M 2006 Mixing with bubbles: a practical technology for use with portable microfluidic devices *Lab on a Chip 6* 207-212 doi :10.1039/b510843h

Glasgow I and Aubry N 2003 Enhancement of microfluidic mixing using time pulsing *Lab on a Chip 3* 114-120

Hessel V, Lowe H and Schonfeld F 2005 Micromixers-a review on passive and active mixing principles *Chemical Engineering Science 60* 2479-2501

Hong C C, Choi J W and Ahn C H 2004 A novel in-plane passive microfluidic mixer with modified Tesla structures, Miniaturization for chem *Biology & Bioeng Lab Chip 4* 109-113

Hossain S, Ansari M A and Kim K Y 2009 Evaluation of the mixing performance of three passive micromixers *Chemical Engineering Journal 150* 492-501

Kamholz A E et al 1999 Quantiative analysis of molecular interactive in microfluidic channel: the T-sensor *Anal. Chem. 71* 5340-7

Kim K Y and Ansari M A 2007 Shape optimization of a micromixer with staggered herringbone groove *Chemical Engineering Science 62* 6687-6695 doi: 10.1016/j.ces.2007.07.059

Kim K Y, Hossain S and Husain A 2010 Shape optimization of a micromixer with staggered-herringbone

grooves patterned on opposite walls *Chemical Engineering Journal 162* 730- 737 doi: 10.1016/j.cej.2010.05.056

Lee S W and Lee S S 2008 Rotation effect in split and recombination micromixing *Sensors and Actuators B 129* 364- 371

Li L, Lee L J, Castro J M and Yi A Y 2010 Improving mixing efficiency of a polymer micromixer by use of a plastic shim divider *J. Micromech. Microeng. 20* 035012 9pp doi: 10.1088/0960-1317/20/3/035012

Liu R H et al 2003 Hybridization enhancement using cavitation microstraming *Analytical Chemistry 75* 1911-917

Li Y, Qu S and Guo Z 2011 Fabrication of microfluidic devices in silica glass by water-assisted ablation with femtosecond laser pulses *J. Micromech. Microeng.21* 075008 5pp doi:10.1088/0960-1317/21/7/075008

Mansur E A, Mingxing Y, Yondong W and Youyuan D 2008 A State-of-the-art Review of Mixing in Microfluidic Mixers *Chinese Journal of Chemical Engineering 16 (4)* 503-516

Matsuyama K, Mine K, Hideaki K, Aoki N and Mae K 2010 Optimization methodology of operation of orifice-shaped micromixer based on micro-jet concept *Chemical Engineering Science 65* 5912-5920 doi:10.1016/j.ces.2010.08.013

Matsuyama K, Mine K, Kubo H and Mae K 2011 Design of micromixer for emulsification and application to conventional commercial plant for cosmetic *Chemical Engineering Journal 167* 727-733 doi: 10.1016/j.cej.2010.09.085

Nguyen N T 2008 Micromixers: Fundamentals, Design and Fabrication *William Andrew* Norwich NY USA

Nguyen N T and Wu Z 2005 Micromixers- a review *J. Micromech. Microeng. 15* R1-R16

Nimafar M, Viktorov V and Martinelli M 2012 Experimental comparative mixing performance of passive Micromixers with H-shaped sub-channels *Chemical Engineering Science 76* 37-44 doi: 10.1016/j.ces.2012.03.036

Ohkawa K, Nakamotob T, Izukab Y et al 2008 Flow and mixing characteristics of σ-type plate static mixer with splitting and inverse recombination *Chemical Engineering research and Design 86* 1447-1453

Park J M, Seo K D and Kwon T H 2010 A chaotic micromixer using obstruction-pairs *J. Micromech.*

Microeng. 20 015023 11pp doi: 10.1088/0960-1317/20/1/015023

Scherr T, Quitadamo C, Tesvich P, Park D S W, Tiersch T, Hayes D, Choi J W, Nandakumar K and Monroe W T 2012 A planar microfluidic mixer based on logarithmic spirals *J. Micromech. Microeng.22* 055019 10pp doi: 10.1088/0960-1317/22/5/055019

Sheu T.S., Chen S.J., Chen J.J., 2012. Mixing of a split and recombine micromixer with tapered curved microchannels, Chemical Engineering Science 71, 321-332, doi: 10.1016/j.ces.2011.12.042.

Shih T R and Chung C K 2008 A high-efficiency planar micromixer with convection and diffusion mixing over a wide Reynolds number range *Microfluidic Nanofluidic Journal 5* 175-183 doi:10.1007/s10404-007-0238-4

Sinton D and Coleman J T 2005 A sequentional injection microfluidic mixing strategy *Microfluidic Nanofluidic Journal 1* 319-327 doi: 10.1007/s10404-005-0034-y

Soleymani A, Yousefi H and Turunen I 2008 Dimensionless number for identification of flow patterns inside a T- micromixer *Chemical Engineering Science 63* 5291-5297 doi: 10.1016/j.ces.2008.07.002

Solliec C, Mouheb N A, Montillet A, Malsch D and Henkel T 2012 Numerical and experimental investigations of mixing in T-shaped and cross-shaped micromixers *Chemical Engineering Science 68* 278-289 doi: 10.1016/j.ces.2011.09.036

Song K H, Jung Y J, Park S H and Choe J 2012 Recrystallization of polyethylene submicron particles using a continuous flow micromixer system *Powder Technology 217* 325-329 doi: 10.1016/j.powtec.2011.10.044

Sullivan S P et al 2007 Simulation of miscible diffusive mixing in microchannels *Sensors and Actuators B 123* 1142-1152

Swickratha M J, Burnsa S D and Wnekb G E 2009 Modulating passive micromixing in 2-D microfluidic devices via discontinuities in surface energy *Sensors and Actuators B 140* 656-662

Tofteberg T, Skolimowski M, Andreassen E and Geschke O 2010 A novel passive micromixer: lamination in a planarchannel system *Microfluidic Nanofluidic Volume 8* Number 2 209-215

Wang H, Iovenitti P, Harvey E and Masood S 2003 Numerical investigation of mixing in microchannels with patterned grooves *J. Micromech. Microeng. 13* 801-808

Wang Y, Zhang K, Guo S, Zhao L, Zhao X and Chan H L W 2011 Realization of planar mixing by chaotic

velocity in microfluidics *Microelectronic Engineering 88* 959-963 doi: 10.1016/j.mee.2010.12.029

Wong S H, Ward M C L and Wharton CW 2004 Micro T-mixer as a rapid mixing micromixer *Sensors and Actuators B 100 359-379* doi: 10.1016/j.snb.2004.02.008

Xua Z, Li C, Vadilloc D, Ruanb X and Fub X 2011 Numerical simulation on fluid mixing by effects of geometry in staggered oriented ridges micromixers *Sensors and Actuators B 153* 284-292.

Yang J T, Fang W F and Tung K Y 2008 Fluid mixing in devices with connected-groove channels *J. Chemical Engineering Science 63* 1871-1881 doi: 10.1016/j.ces.2007.12.027

Yang J T, Wang L and Lyu P C 2007 An overlapping crisscross micromixer *J. Chemical Engineering Science 62* 711- 720 doi: 10.1016/j.ces.2006.09.048

Yang S Y, Lin J L and Lee G B 2009 A vortex-type micromixer utilizing pneumatically driven membranes *J. Micromech. Microeng. 19* 035020 9pp doi:10.1088/0960-1317/19/3/035020

Yang Z *et al* 2001 Ultrasonic micromixer for microfluidic systems *Sensors and Actuators A 93* 266-272

Yu X, Lin Y, Wang Z, Tu S T and Wang Z 2011 Design and evaluation of an easily fabricated micromixer with three- dimensional periodic perturbation *Chemical Engineering Journal 171* 291-300 doi: 10.1016/j.cej.2011.04.003

Zimmerman W B and Hassell D G 2006 Investigation of the convective motion through a staggered Herringbone micromixer at low Reynolds number flow *J. Chemical Engineering Science 61* 2977-2985 doi: 10.1016/j.ces.2005.10.068